Methods, and Techniques, pp 1–29, Marcel Dekker, New York.

Haq, H., Christodoulides, L., Ketterer, B., & Shrago, E. (1982) *Biochim. Biophys. Acta 713*, 193–198.

Hunt, C. R., Ro, J. H., Dobson, D. E., Min, H. Y., & Spiegelman, B. M. (1986) *Proc. Natl. Acad. Sci. U.S.A. 83*, 3786–3790.

Jones, T. A., Bergfors, T., Sedzik, J., & Unge, T. (1988) *EMBO J. 7*, 1597–1604.

Keuper, H. J. K., Klein, R. A., & Spener, F. (1985) *Chem. Phys. Lipids 38*, 159–173.

Konev, S. V. (1967) *Fluorescence and Phosphorescence of Proteins and Nucleic Acids* (Undenfriend, S., translator) pp 9–39, Plenum Press, New York.

Lakowicz, J. R. (1983) *Principles of Fluorescence Spectroscopy*, pp 257–274, Plenum Press, New York.

Matarese, V., & Bernlohr, D. A. (1988) *J. Biol. Chem. 263*, 14544–14551.

Matayoshi, E. D., & Kleinfeld, A. M. (1981) *Biophys. J. 35*, 215–235.

Ockner, R. K., Manning, J. A., & Kane, J. P. (1982) *J. Biol. Chem. 257*, 7872–7878.

Offner, G. D., Troxler, R. F., & Brecher, P. (1986) *J. Biol. Chem. 261*, 5584–5589.

Parker, C. A., & Rees, W. T. (1960) *Analyst 85*, 587–600.

Paulussen, R. J. A., Jansen, G. P. M., & Veerkamp, J. H. (1986) *Biochim. Biophys. Acta 877*, 342–349.

Podo, F., & Blasie, J. K. (1977) *Proc. Natl. Acad. Sci. U.S.A. 74*, 1032–1036.

Sacchettini, J. C., Said, B., Schulz, H., & Gordon, J. I. (1986) *J. Biol. Chem. 261*, 8218–8223.

Sacchettini, J. C., Gordon, J. I., & Banaszak, L. J. (1988) *J. Biol. Chem. 263*, 5815–5819.

Sacchettini, J. C., Gordon, J. I., & Banaszak, L. J. (1989) *J. Mol. Biol. 208*, 327–339.

Said, B., & Schulz, H. (1984) *J. Biol. Chem. 259*, 1155–1159.

Scott, T. G., Spencer, R. D., Leonard, N. J., & Weber, G. (1970) *J. Am. Chem. Soc. 92*, 687–695.

Spencer, R. D., & Weber, G. (1969) *Ann. N.Y. Acad. Sci. 158*, 361–376.

Spiegelman, B. M., & Green, H. (1980) *J. Biol. Chem. 255*, 8811–8818.

Spiegelman, B. M., Frank, M., & Green, H. (1983) *J. Biol. Chem. 258*, 10083–10089.

Storch, J., & Bass, N. M. (1990) *J. Biol. Chem. 265*, 7827–7831.

Storch, J., & Schachter, D. (1985) *Biochim. Biophys. Acta 812*, 473–484.

Storch, J., Bass, N. M., & Kleinfeld, A. M. (1989) *J. Biol. Chem. 264*, 8708–8713.

Sweetser, D. A., Heuckeroth, R. O., & Gordon, J. I. (1987) *Annu. Rev. Nutr. 7*, 337–359.

Teale, F. W. J. (1960) *Biochem. J. 76*, 381–388.

Tilley, L., Thulborn, K. R., & Sawyer, W. H. (1979) *J. Biol. Chem. 254*, 2592–2594.

Thulborn, K. R., & Sawyer, W. H. (1978) *Biochim. Biophys. Acta 511*, 125–140.

Thulborn, K. R., Tilley, L. M., Sawyer, W. H., & Treloar, F. E. (1979) *Biochim. Biophys. Acta 558*, 166–178.

Veerkamp, J. H., & Paulussen, R. J. A. (1987) *Biochem. Soc. Trans. 15*, 331–336.

Vincent, M., de Foresta, B., Gallay, J., & Alfsen, A. (1982) *Biochemistry 21*, 708–716.

Vork, M. M., Glatz, J. F. C., Surtel, D. A. M., & Van der-Vusse, G. J. (1990) *Mol. Cell. Biochem.* (in press).

Waggoner, A. S., & Stryer, L. (1970) *Proc. Natl. Acad Sci U.S.A. 67*, 579–589.

Werner, T. C. (1976) in *Modern Fluorescence Spectroscopy* (Wehry, E. L., Ed.) Vol. 2, pp 277–317, Plenum Press, New York.

Werner, T. C., & Hoffman, R. M. (1973) *J. Phys. Chem. 77*, 1611–1615.

Werner, T. C., Matthews, T., & Soller, B. (1976) *J. Phys. Chem. 80*, 533–541.

Zezulak, K. M., & Green, H. (1985) *Mol. Cell. Biol. 5*, 419–421.

Multiple Heme Pocket Subconformations of Methemoglobin Associated with Distal Histidine Interactions

A. Levy, P. Kuppusamy, and J. M. Rifkind*

Laboratory of Cellular and Molecular Biology, National Institute on Aging, Gerontology Research Center, National Institutes of Health, Baltimore, Maryland 21224

Received March 15, 1990; Revised Manuscript Received June 14, 1990

ABSTRACT: Electron paramagnetic resonance spectra of methemoglobin reveal that, in addition to the major tetragonal high-spin aqueous complex and the low-spin hydroxide complex, three other complexes associated with the interaction of the distal histidine are resolved. These are a rhombic high-spin and two classes of low-spin bis-histidine complexes. By freeze-quenching experiments it is shown that the rhombic high-spin and one of the low-spin bis-histidine complexes (B) are at equilibrium with the dominant species. Incubation in the 210–260 K temperature range shifts the total equilibrium toward a low-energy state with the distal histidine coordinated to the iron (complex C).

On the distal side of the heme pointing into the ligand pocket on almost all mammalian hemoglobins and myoglobins is a histidine, the distal histidine. The role of this histidine has been discussed by many investigators (Giacometti et al., 1980; Mims et al., 1983; Tucker et al., 1978; Shaanan, 1983; Rifkind, 1988). It has been suggested that the histidine acts

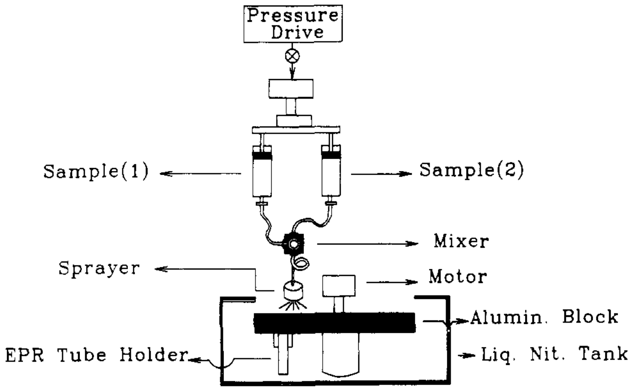

FIGURE 1: Freeze–quenching apparatus.

like a gate, which sterically hinders the access into the ligand pocket (Case & Karplus, 1979), thereby regulating ligand binding kinetics. Moreover, after ligation, the protein may assume a subconformation where the distal histidine stabilizes the ligand binding by forming a hydrogen bond with the axial ligand. This subconformation was observed in the α-chains of oxyhemoglobin (Shaanan, 1983) and has been proposed for the bonding of a number of other ligands (Mims et al., 1983; Asher et al., 1981; Anusiem et al., 1968; Beetlestone & Irvine, 1969).

Although the X-ray data indicate that the distal histidine is located more than 4 Å away form the iron, there have been a number of reports in the literature for complexes involving the distal histidine and the iron (Mayo et al., 1983; Papaefthymiou et al., 1975; Peisach et al., 1973; Rein et al., 1971). For the most part these complexes have been attributed to denatured nonfunctional forms of hemoglobin.

We have previously (Levy et al., 1982, 1984; Levy & Rifkind, 1985) reported enhanced formation of several classes of bis-histidine complexes at subzero temperatures in the absence of axial ligands, i.e., deoxyhemoglobin, or with weak axial ligands like H_2O in methemoglobin. The complexes were demonstrated to be thermally accessible low-entropy subconformations of hemoglobin. It was further shown that the rate of formation of this subconformation could be used to monitor the heme pocket flexibility (Levy & Rifkind, 1985). In these studies a low concentration of the bis-histidine complexes was already detected in the instantly frozen deoxyhemoglobin and methemoglobin samples. The results imply a finite occupancy of this subconformation at room temperature and consequently a conceivable functional role. The short distance required for bond formation between the iron and the N of the distal histidine does not contradict the X-ray data when it is recognized that proteins exist in multiple subconformations (Frauenfelder et al., 1979). The raw X-ray data yield a Boltzmann weighted average of the various subconformations. Therefore, the refinement usually results with the coordinates of the most probable subconformation, ignoring other subconformations irrespective of their functional significance.

The original Mössbauer studies (Levy & Rifkind, 1985) were performed on 1-mL samples in Lucite holders submerged in liquid nitrogen for fast freezing. This procedure results in a relatively long freezing time, permitting conformational redistribution during the freezing process. In addition, the ^{57}Fe-reconstituted hemoglobin used in these studies could be more susceptible to bis-histidine complex formation (Yamamoto & LaMar, 1986).

In this paper we have utilized a freeze–quenching technique (Figure 1) and EPR to study the methemoglobin bis-histidine complexes present immediately after freezing and those formed in the frozen state. The freeze–quenching system made it possible to provide a more reliable reflection of the different subconformations present at room temperature.

EXPERIMENTAL PROCEDURES

Human erythrocytes were obtained through the Baltimore Longitudinal Study of Aging at the Gerontology Research Center. The cells were washed several times by suspending them in 0.9% NaCl and recentrifuging them. The cells were then hemolyzed in 2 volumes of distilled water at 4 °C and separated from the cell membranes by high-speed centrifugation. Complete removal of the membranes was facilitated by freezing and thawing the hemolysate prior to centrifugation. The low molecular weight components were removed by dialysis and gel filtration on Sephadex G-25 eluted at 4 °C with 0.01 M Trizma–0.1 M NaCl, pH 7.4, buffer.

Hemoglobin was oxidized to form methemoglobin by a 5-fold excess of ferricyanide, which was then removed by exhaustive dialysis. X-band EPR spectra were measured by using an IBM ER-200D-SRC spectrometer with 100-kHz modulation and an Air Products Model LTD-3-110 liquid-transfer Heli-Tran cryogenic unit with an APD-E temperature controller. Diphenylpicrylhydrazyl (DPPH) was used as a g marker.

Quartz EPR sample tubes (4 mm; Wilmad) were used. The samples were frozen by one of two ways: (1) The EPR tube was submerged directly into liquid nitrogen. Breakage of the tube was prevented by insertion into the quartz tube of a thin polyethylene tube sealed at the bottom. (2) Freeze–quenching was performed with a specially designed apparatus (Figure 1). The sample was sprayed directly on a spinning aluminum block at liquid nitrogen temperature. The frozen sample was then collected into a groove on the block and packed directly into the EPR tube which was attached underneath the aluminum block protruding out of a hole in the groove.

The quenching time calibration was obtained by freeze–quenching a mixture of NaF and methemoglobin at pH 6.0 driven from syringe 1 and syringe 2, respectively (see Figure 1). The EPR spectrum of the frozen mixture displayed less than 5% reaction. On the basis of a second-order rate constant of 26 s^{-1} mol^{-1} (Gibson et al., 1969) a quenching time of less than 10 ms is indicated.

This apparatus has several advantages over the previously used EPR freeze–quenching apparatus (Bray, 1961; Bray et al., 1973; Rifkind, 1979). These include a faster quenching time, no need for an isopentane bath, and easier transfer to the EPR tube.

The EPR samples were stored in liquid nitrogen until the spectrum was run at 12 K. Incubations at 233 and 213 K were performed by removing the EPR sample tube from the cavity and placing in a bath of the appropriate temperature for the designated time. Because of the time required for temperature equilibration of the sample, the shortest incubation times used were 1 min.

RESULTS

EPR Spectra of Human Methemoglobin. Figure 2 shows the 12 K EPR spectrum of a freshly prepared human methemoglobin (0.05 M Bis-Tris, pH 6.5). In this spectrum one can delineate a number of bands which can be assigned to five iron complexes: a high-spin tetragonal complex characterized by a band with lines at $g_\perp = 6.0$ and $g_\parallel = 2.0$; a high-spin rhombic complex for which the only resolved band is $g = 4.3$; a low-spin band (A) attributed to the hydroxide complex with $g_1 = 2.59$, $g_2 = 2.17$, and $g_3 = 1.83$; as well as two other low-spin complexes (B and C). Complex B has $g_1 = 2.83$, $g_2 = 2.26$, and $g_3 = 1.63$. Complex C is most easily detected by

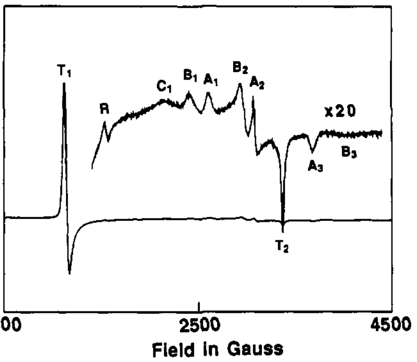

FIGURE 2: EPR spectrum of methemoglobin at pH 7.6. Frozen by submerging tube in liquid nitrogen. T_1 and T_2 are $g_\perp$ and $g_\parallel$ components of the tetragonal high-spin complex, respectively. R represents the signal of the rhombic high spin; A_i, B_i, and C_i are signals originating from low-spin complexes A, B, and C, respectively, and i represents the respective g_i component (see text).

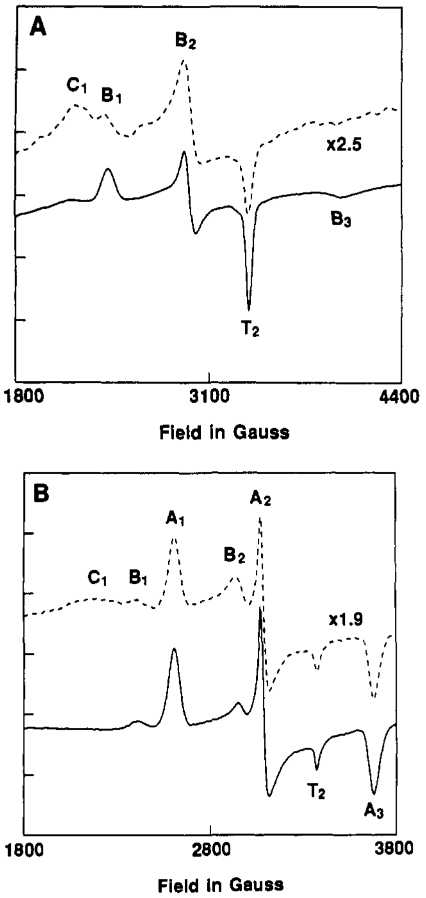

FIGURE 3: EPR spectrum of methemoglobin, cooled by the freeze-quenching apparatus. (A) pH 6.4 sample: (—) sample stored at liquid nitrogen; (---) sample incubated for 20 min at 233 K. (B) pH 8.9 sample: (—) sample stored at liquid nitrogen; (---) sample incubated for 20 min at 233 K.

the low-field g_1 line (2.98). For this complex $g_2 = 2.28$, slightly higher than that of component B (see below), and the corresponding g_3 line which would have a much lower signal height is not detected. Although the three low-spin complexes result in overlapping or partly undetectable EPR bands, they are readily discernible in the low-field g_1 region. Thus the relative intensities of the g_1 EPR signals are consistently used in this work to evaluate the relative concentration of the respective complexes.

The quenched samples in Figure 3 show the effect of raising the pH from 6.4 to 8.9 on the EPR spectrum. One can observe a concurrent decrease of the high spin ($g_\parallel$ signal) and the low-spin complex B with an increase in the hydroxide A component as the pH is elevated. It is important to note that the relative concentration of complex B and the high spin as measured by the intensity ratio of the B_1 and $g_\parallel$ signals were found to be unchanged in this pH range.

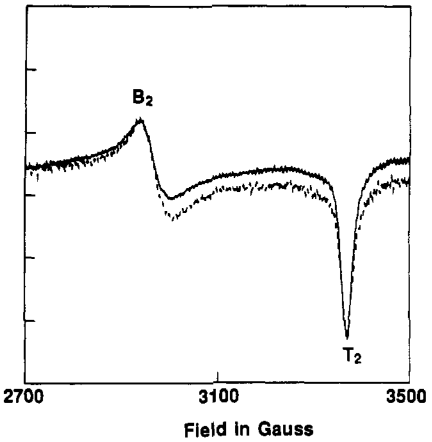

FIGURE 4: Effect of ambient temperature prior to quenching on the EPR spectrum of methemoglobin: (—) initial temperature 310 K; (---) initial temperature 278 K.

Figure 4 shows an EPR spectrum overlap of two pH 6.4 methemoglobin samples quenched in liquid nitrogen from initial temperatures of 310 and 278 K. The spectra delineate the B_2 and $g_\parallel$ lines of complex B and the high-spin complex, respectively. Comparison of the two spectra indicate a relative increase of complex B for the sample quenched from lower temperature.

Time-Dependent Redistribution of Methemoglobin Components. Panels A and B of Figure 3 show the effect of 20-min incubation at 233 K on freezed-quenched human methemoglobin at pH 6.4 and 8.9, respectively. At pH 6.4 both complexes B and the high spin ($g_\parallel$) diminished upon incubation with a simultaneous increase in complex C. It is important to note that the amount of complex C detected in the freeze-quenched sample was greatly reduced when compared with samples submerged in liquid nitrogen (compare to Figures 2 and 3). At pH 8.9 the increase in the concentration of component C is concurrent with the decrease in the intensity of the EPR signal of the hydroxide complex A. Both panels A and B of Figure 3 indicate that component C becomes a major component after the 20-min incubation. The pH and incubation dependence of the EPR spectra confirm the assignment of the bands associated with each complex (see above). A decrease of the rhombic high spin similar to that of the tetragonal high-spin and low-spin A and B occurs.

The redistribution among methemoglobin complexes with the formation of complex C is highly temperature dependent, with essentially no change detected below 170 K. At 233 K, used for the incubation studies in Figure 3, approximately 90% of the redistribution between the methemoglobin states is completed within 2 min. In order to obtain additional information concerning the interconversion, time-dependent studies were performed at the lower temperature of 213 K.

Figure 5 displays the EPR spectra in the low-spin g_1 region (from 2000 to 2800 G) of human methemoglobin at pH 6.4 subjected to various incubation times at 213 K. At this temperature the interconversion is much slower with only a partial conversion even after 60 min. Under this condition it is possible to discern not only changes in intensity but also changes in the shape of the spectra for component C as a function of incubation time, suggesting the existence of multiple C type complexes. Further evidence for multiple C

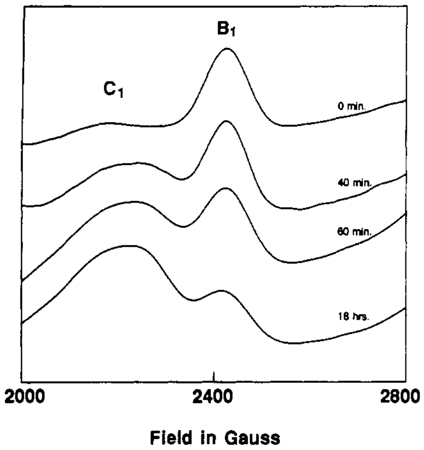

FIGURE 5: Evolution of the EPR spectrum of methemoglobin at pH 6.4 incubation for various times at 213 K. Spectra depict the formation of complex C as expressed by the EPR signal of its g_1 component.

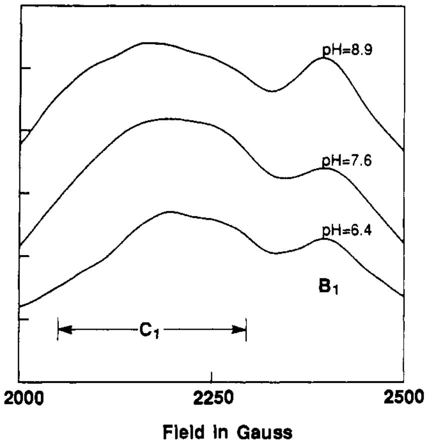

FIGURE 6: Effect of pH on the EPR spectrum of the low-spin g_1 component of methemoglobin after 20-min incubation at 233 K.

type complexes is indicated by expanded spectra of human methemoglobin at various pH's incubated for 20 min at 233 K (Figure 6).

Figure 7 shows a comparison of the EPR spectra of horse and human methemoglobin at pH 6.4 after low-temperature incubation. One can note the same B type complex and heterogenous C type complex for both methemoglobins. In both species the C type g_1 signal consists of similar multiple lines spread out between $g = 2.9$ and 3.1 for the different subcomponents. However, disparities between horse and human species are observed in the line width and the relative intensities of the subcomponents which can be attributed to subtle differences between the heme pockets.

DISCUSSION

Nature of the Methemoglobin Complexes. The 6-fold degenerate $S = {}^5/_2$ state of high-spin Fe(III) splits into three Kramers' doublets in the presence of a crystal field (Blumberg, 1967; Golding, 1977). The EPR spectrum is therefore a Boltzmann weighted superposition of three spectral components. For powder samples and tetragonal symmetry two signals at $g_\perp = 6$ and $g_\parallel = 2$ originating from the lowest Kramers' doublet dominate the EPR spectrum. However, rhombic distortion splits the ground-state signal, and the observed spectrum consists of a signal arising from the middle Kramers' doublet with $g = 4.3$.

Although hemoglobin generally produces high-spin tetragonal complexes, rhombic distortion has been reported for isolated α-chains (Peisach et al., 1969), for abnormal hemoglobin M's (Hayashi et al., 1967) where the distal histidine is replaced by tyrosine, and in other heme proteins (Peisach et al., 1971). A minor rhombic component with $g = 4.3$ is observed for all methemoglobin samples (Figure 2).

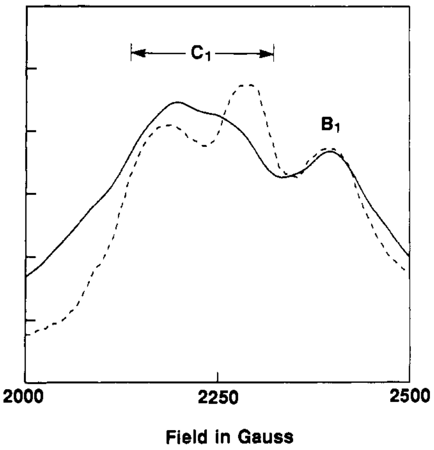

FIGURE 7: Comparison of human and horse methemoglobin in the low-spin g_1 region of the EPR spectrum: (—) human methemoglobin, pH 6.4; (- - -) horse methemoglobin, pH 6.4.

The distortion of the octahedral symmetry around the Fe(III) in low-spin $S = {}^1/_2$ heme complexes yields three lines in the EPR spectrum. From the g values of the three lines, using the single-hole Griffith model (Griffith, 1956; Bohan, 1977), it is possible to calculate the tetragonal (V) and rhombic (Δ) splitting of the ligand field. On the basis of the value of V/λ and Δ/λ, where λ is the spin orbit coupling parameter, Blumberg and Peisach (1971a,b) have categorized low-spin heme complexes into five classes (P, O, B, H, and C), each identified with a specific ligand. The EPR parameters of low-spin complexes A–C have been used to identify the sixth ligand coordinated to the heme iron.

Complex A has ligand field parameters $V/\lambda = 3.32$ and $\Delta/\lambda = 6.29$ consistent with class O complexes for an oxygen ligand coordinated to the heme. The g values of this complex are identical with those attributed to the binding of hydroxide to methemoglobin (Yonetani et al., 1971).

Complex B has ligand field parameters $V/\lambda = 2.20$ and $\Delta/\lambda = 3.71$ of class H, which are attributed to a complex with two nitrogenous axial ligands. This complex is presumably associated with the coordination of the distal histidine in the ligand pocket with the iron. The relative signal intensity of B decreases below pH 6 where the histidine is expected to protonate. This observation supports the coordination of the distal histidine in complex B. Similar EPR parameters have been previously reported in low-pH methemoglobin samples at liquid helium temperatures (Yonetani et al., 1971). The EPR spectra were attributed to the formation of a complex with distal histidine. An analogous ligation to the distal histidine at low temperatures was observed in Mössbauer studies on deoxyhemoglobin (Levy & Rifkind, 1985).

Complex C. From the two g values determined for complex C it is possible to calculate the third (Griffith, 1956) as well as the ligand field parameters $V/\lambda = 1.69$ and $\Delta/\lambda = 2.75$. This complex has g values similar to those found for the imidazole complex of methemoglobin with ligand field parameters of class B also associated with complexes with two nitrogenous ligands. Complex C is therefore also identified with the coordination of the distal histidine to methemoglobin.

The distinct EPR parameters for the C and B complexes could be associated with a change in the length of the N–Fe bond which would be expected to influence the ligand donor strength, or perhaps more readily, changes in the orientation of the distal imidazole ring (Dervartanian & Legall, 1978; Higuichi et al., 1983; Palmer, 1985). Because the fifth and the sixth ligands of the histidine complexes are part of the protein matrix, subtle changes in the pocket conformation result in changes in the geometry of the heme complexes and the EPR spectrum, which are generally not resolved with exogenous ligands. It is this sensitivity to the pocket conformation which produces both B and the multiple C type components observed in Figures 5–7.

High Spin–Low Spin Equilibria. Methemoglobin hydroxide, like many of the other methemoglobin complexes, exists at room temperature as a mixture of high spin and low spin (Beetlestone & George, 1964; Iizuka & Kotani; 1969). However, the equilibrium is shifted to the low-spin form as the temperature is lowered. At liquid nitrogen temperature and below, only the low-spin complex is detected. Complex A thus represents all of the methemoglobin hydroxide.

Complex B reflects a subconformation that is present at room temperature and is not formed during the freezing process. Thus the highest concentration of complex B is found in the samples prepared by freeze–quenching where the room temperature distribution of the different species is preserved. However, the same proportional decrease observed in the EPR signal intensity of the high-spin aqueous complex and that of complex B as the pH is increased (Figure 3) implies an equilibrium between both species. Of these two complexes a higher energy state is assigned to the high-spin aqueous complex since an increase in the relative signal intensity of complex B to that of the high spin is observed in the samples quenched from lower initial temperature. Therefore, a temperature-dependent spin equilibrium exists between the high-spin aqueous complex and complex B analogous to that of the hydroxide complex.

Nevertheless, the energy barrier of the high spin → low spin transition is larger for the low-pH water complex than the high-pH hydroxide complex. Thus the hydroxide complex is considered to be completely in the low-spin form (Iizuka & Kutani, 1969) even for samples quenched from room temperature. The small amount of high-spin complex at pH 8.9 (Figure 3B) is presumably associated with that small fraction of hemoglobin with water bound. For the water complex at low pH no changes are detected below 170 K, and even at 213 K the conversion to low-spin B is slower than the conversion from B to C (Figure 5).

This distinction can be attributed to a qualitative difference in the nature of the spin transition. While only a spatial electron density redistribution is required in the hydroxide spin transitions, a supplementary movement of the distal histidine is necessary for the formation of complex B, which dictates a larger energy barrier for the transition.

Low-Temperature Bis-Histidine Subconformations. Low-temperature incubation transforms methemoglobin into C type complex. This partial transformation involves both low-spin A and B and the high-spin complex. At 233 K most of A and B and approximately 50% of the high spin are transformed into complex C; this complex is the dominant methemoglobin species at low temperature. This observation is consistent with magnetic susceptibility studies on methemoglobin subjected to slow cooling (Iizuki & Kotani, 1969; Yonetani et al., 1971).

The formation of complex C at temperatures as low as 215 K excludes changes in the energy barriers caused by the freezing of the hydration shell which is known to be already frozen at 240 K (Keller & Debrunner, 1980). Complex C instead must reflect a low-energy state within the conformational substates of native methemoglobin. In the absence of exogenous sixth ligand, or in the presence of weak exogenous ligands like water, the gain in enthalpy associated with the binding of the distal histidine is able to compensate for the loss in entropy associated with fixing the geometry of the distal histidine relative to the heme. A similar explanation has been proposed for the formation of bis-histidine complex in deoxyhemoglobin (Levy & Rifkind, 1985).

The multiple C type complexes (Figures 5–7) imply subtle differences in the pocket conformation with similar energies. However, the conversion from the B type bis-histidine complex at low temperature implies that complex C is energetically favored. The heme pocket configuration of the higher energy bis-histidine complex B is suggested by the dependence on pH (Figure 3) and the rapid equilibrium at room temperature (Figure 4). These results are consistent with the complex B configuration in which a water molecule is still retained in the ligand pocket. The presence of water would be incompatible with the energetically most stable configuration for the bis-histidine complex (complex C). The requirement for water to leave the pocket slows down the conversion from B to C, particularly at low temperatures where the egress of ligands from the pocket becomes extremely slow.

CONCLUSION

Recent studies have emphasized the potential importance of distinct subconformations in explaining protein fluctuations. Unfortunately, it is frequently difficult to obtain experimental data of these different subconformations and the activation energies between them. By using freeze–quenching combined with the sensitivity of EPR to the distal histidine coordination and the geometry of this bis-histidine complex, it has been possible to delineate several of these subconformations within the heme pocket where ligand binding occurs and to study the interconversion between them. These processes must be considered in delineating hemoglobin binding dynamics.

REFERENCES

Anusiem, A. C., Beetlestone, J. G., & Irvine, D. H. (1968) *J. Chem. Soc. A*, 960–969.

Asher, S. A., Adams, M. L., & Schuster, T. M. (1981) *Biochemistry 20*, 3339–3346.

Beetlestone, J., & George, P. (1964) *Biochemistry 3*, 707–714.

Beetlestone, J. G., & Irvine, D. H. (1969) *J. Chem. Soc. A.*, 735–742.

Blumberg, W. E. (1967) in *Magnetic Resonance in Biological Systems* (Ehrenberg, A., Malmström, B. G., & Vänngåard, T., Eds.) pp 119–133, Pergamon Press, Oxford, England.

Blumberg, W. E., & Peisach, J. (1971a) in *Probes of Structure and Function of Macromolecules and Membranes, Volume II, Probes of Enzymes and Hemoproteins* (Chance, B., Yonetani, T., & Mildvan, A. S., Eds.) pp 215–229, Academic Press, New York.

Blumberg, W. E., & Peisach, J. (1971b) in *Bioinorganic Chemistry* (Gould, R. F., Ed.) Advances in Chemistry Series 100, pp 271–291, American Chemical Society, Washington, DC.

Bohan, T. L. (1977) *J. Magn. Reson. 26*, 109–118.

Bray, R. C. (1961) *Biochem. J. 81*, 189–193.

Bray, R. C., Lowe, D. J., Capeillerê-Blandin, C., & Fielden, E. M. (1973) *Biochem. Soc. Trans. 1*, 1067–1072.

Case, D. A., & Karplus, M. (1979) *J. Mol. Biol. 132*, 343–368.

Dervartanian, D. V., & Legall, T. (1978) *Biochim. Biophys. Acta 502*, 458–465.

Frauenfelder, H., Petsko, G. A., & Tsernoglou, D. (1979) *Nature (London) 280*, 558–563.

Giacometti, G. M., Brunori, M., Antonini, E., DiIorio, E. E., & Winterhalter, K. H. (1980) *J. Biol. Chem. 255*, 6160–6165.

Gibson, Q. H., Parkhurst, L. J., & Geraci, G. (1969) *J. Biol. Chem. 244*, 4668–4676.

Golding, R. M., Singhasowich, T., & Tennant, W. C. (1977) *Mol. Phys. 34*, 1343–1350.

Griffith, J. S. (1956) *Proc. R. Soc. London, A 235*, 23–36.

Hayashi, A., Suzuki, T., Shimizu, A., Morimoto, H., & Watari, H. (1967) *Biochem. Biophys. Acta 147*, 407–409.

Higuchi, Y., Kusunoki, M., Matsuura, Y., Yasuoka, N., & Kakudo, M. (1984) *J. Mol. Biol. 172*, 109–139.

Iizuka, T., & Kotani, M. (1969) *Biochem. Biophys. Acta 194*, 351–363.

Keller, H., & Debrunner, P. G. (1980) *Phys. Rev. Lett. 45*, 68–71.

Levy, A., & Rifkind, J. M. (1985) *Biochemistry 24*, 6050–6054.

Levy, A., Walker, J. C., & Rifkind, J. M. (1982) *J. Appl. Phys. 53*, 2066–2068.

Levy, A., Alston, K., & Rifkind, J. M. (1984) *J. Biomol. Dyn. 1*, 1299–1309.

Mayo, K. H., Kucheida, D., Parak, F., & Chien, J. C. W. (1983) *Proc. Natl. Acad. Sci. U.S.A. 80*, 5294–5296.

Mims, M. P., Porras, A. L., Olson, J. S., Noble, R. N., & Peterson, J. P. (1983) *J. Biol. Chem. 258*, 14219–14232.

Palmer, G. (1985) *Biochem. Soc. Trans. 13*, 548–560.

Papaefhtymiou, G. C., Huynh, B. H., Yens, C. S., Groves, J. L., & Wu, C. S., (1975) *J. Chem. Phys. 62*, 2995–3001.

Peisach, J., Blumberg, W. E., Wittenberg, B. A., Wittenberg, J. B., & Kampa, L. (1969) *Proc. Natl. Acad. Sci. U.S.A. 63*, 934–939.

Peisach, J., Blumberg, W. E., Ogawa, S., Rachmilewitz, E. A., & Oltzik, R. (1971) *J. Biol. Chem. 246*, 3342–3355.

Peisach, J., Blumberg, W. E., & Adler, A. (1973) *Ann. N.Y. Acad. Sci. 206*, 310–327.

Rein, H., Ristau, O., Janig, G. R., & Jung, F. (1971) *FEBS Lett. 15*, 21–23.

Rifkind, J. M. (1979) *Biochemistry 18*, 3860–3865.

Rifkind, J. M. (1988) in *Heme Proteins* (Eichhorn, G. L., & Marzilli, L. G., Eds.) Advances in Inorganic Biochmistry 7, pp 155–245, Elsevier, New York.

Shaanan, B. (1983) *J. Mol. Biol. 171*, 31–59.

Tucker, P. W., Phillips, S. E. V., Perutz, M. F., Houtchens, R., & Caughey, W. S. (1978) *Proc. Natl. Acad. Sci. U.S.A. 75*, 1076–1080.

Yamamoto, Y., & LaMar, G. N. (1986) *Biochemistry 25*, 5288–5297.

Yonetani, T., Iizuka, T., & Waterman, M. R. (1971) *J. Biol. Chem. 246*, 7683–7689.

Small-Angle Scattering Studies Show Distinct Conformations of Calmodulin in Its Complexes with Two Peptides Based on the Regulatory Domain of the Catalytic Subunit of Phosphorylase Kinase[†]

J. Trewhella,[*,‡] D. K. Blumenthal,[§] S. E. Rokop,[‡] and P. A. Seeger[‡]

Life Sciences and Physics Divisions, Los Alamos National Laboratory, Los Alamos, New Mexico 87545, and Department of Biochemistry, University of Texas Health Center at Tyler, Tyler, Texas 75710

Received March 30, 1990; Revised Manuscript Received June 14, 1990

ABSTRACT: Small-angle X-ray and neutron scattering have been used to study the solution structures of calmodulin complexed with synthetic peptides corresponding to residues 342–366 and 301–326, designated PhK5 and PhK13, respectively, in the regulatory domain of the catalytic subunit of skeletal muscle phosphorylase kinase. The scattering data show that binding of PhK5 to calmodulin induces a dramatic contraction of calmodulin, similar to that previously observed when calmodulin is complexed with the calmodulin-binding domain peptide from rabbit skeletal muscle myosin light chain kinase. In contrast, calmodulin remains extended upon binding PhK13. In the presence of both peptides, calmodulin also remains extended. Apparently, the presence of PhK13 inhibits calmodulin from undergoing the PhK5-induced contraction. These data indicate that there is a fundamentally different type of calmodulin–target enzyme interaction in the case of the catalytic subunit of phosphorylase kinase compared with that for myosin light chain kinase.

Calmodulin is an intracellular Ca^{2+}-binding protein involved in a large number of Ca^{2+}-dependent processes. Structural data on calmodulin and its complexes with its many target enzymes are critical for understanding the molecular basis for how each target enzyme is regulated. The three-dimensional crystal structure of calmodulin has been determined (Babu et al., 1985) and was recently refined to 2.2-Å resolution (Babu et al., 1988). The crystallographic data show many important structural details thought to be important for target enzyme interactions including an eight-turn solvent-exposed α-helix connecting two globular lobes, with each lobe containing two Ca^{2+}-binding domains and a solvent-exposed hydrophobic patch. Although this structure is of high resolution, it may not accurately reflect the structure of the protein when in solution, which is most relevant to questions concerning target enzymic interactions. Indeed, CD[1] studies indicate there is

---

[†] This work was performed under the auspices of the DOE (Contract W-7405-ENG-36) and was supported by NIH Grants GM40528 (J.T.), GM39290 (D.K.B.), DOE Project KP-04-01-00-0 (J.T.), and a Grant-In-Aid from the American Heart Association (D.K.B). This work has benefited from the use of facilities at the Manuel Lujan, Jr., Neutron Scattering Center, a national user facility funded as such by the DOE/Office of Basic Energy Sciences.

[*] Address correspondence to this author at the Life Sciences Division, Los Alamos National Laboratory.

[‡] Los Alamos National Laboratory.

[§] University of Texas.

0006-2960/90/0429-9316$02.50/0